Oxide thermoelectrics
From material property to device architecture

Reshma Krishnan Madathil
Centre for Materials Science and Nanotechnology (SMN)
Department of Chemistry
University of Oslo
reshma.madathil@smn.uio.no

THERMiO workshop (09/03/2020)

UiO : Centre for Materials Science and Nanotechnology
University of Oslo

THERMiO
UiO innovation cluster

History of Oxide thermoelectrics

In_2O_3-SnO_x

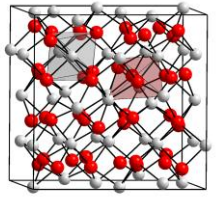

1991

$CaMnO_3$

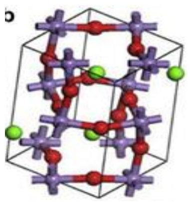

1994

Al-ZnO

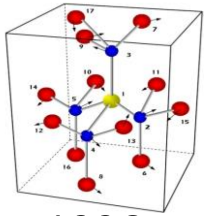

1996

$NaCoO_2$

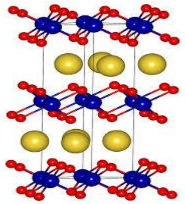

1998

$Ca_3Co_4O_9$

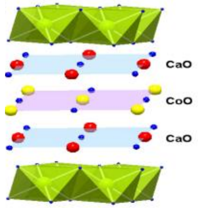

2001

$SrTiO_3$

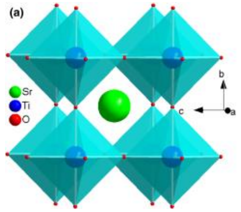

2004

In_2GeO_3

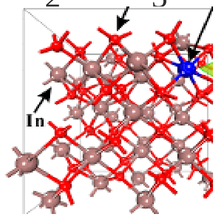

2008

$Zn_{0.96}Al_{0.02}Ga_{0.02}O$

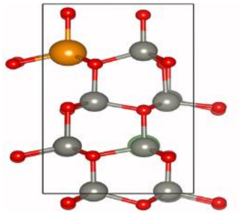

2009

BiCuSeO

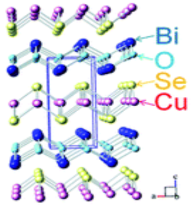

2010

$SrPbO_3$

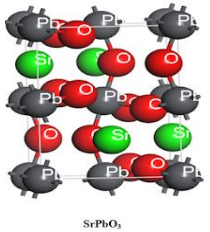

2010

SnO

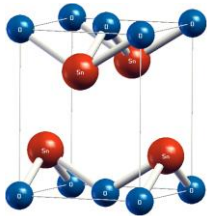

2017

$LaCuO_4$

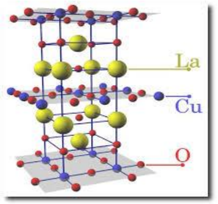

$LaNiO_3$

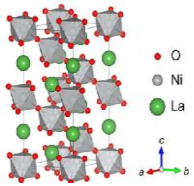

2018

ZT

Next ???

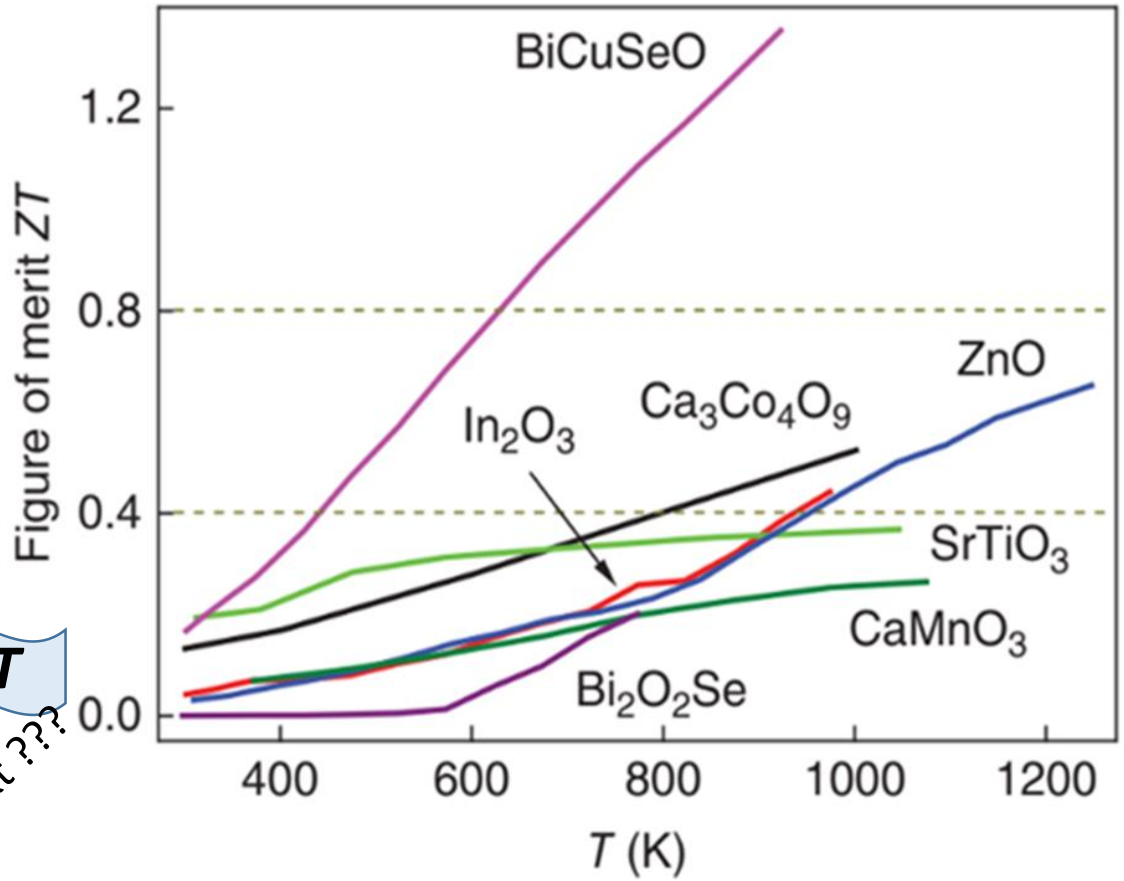

Oxide Thermoelectric Materials, john Wiley & Sons, **2019**

"Phonon-glass electron-crystal" (or PGEC in short),which means that the materials should have a low lattice thermal conductivity as in a glass, and a high electrical conductivity as in a crystals

Strategies to tune and alter TE parameters

- ❑ Optimizing Carrier Concentration
  - incorporation of dopants and altering of stoichiometry
- ❑ Tuning the band structure /Electron band structure engineering
  -Seebeck coefficients are higher in multiple band systems than those with single-band
- ❑ Nanostructure Engineering
  -Phonon scattering by nano-engineering-suppressing the lattice thermal conductivity
- ❑ Manipulating the Defects
  -The First Strategy of Reducing κ_L: Creating Structural Disorders
- ❑ Composites
  -Improved electronic properties and reduced κ_L

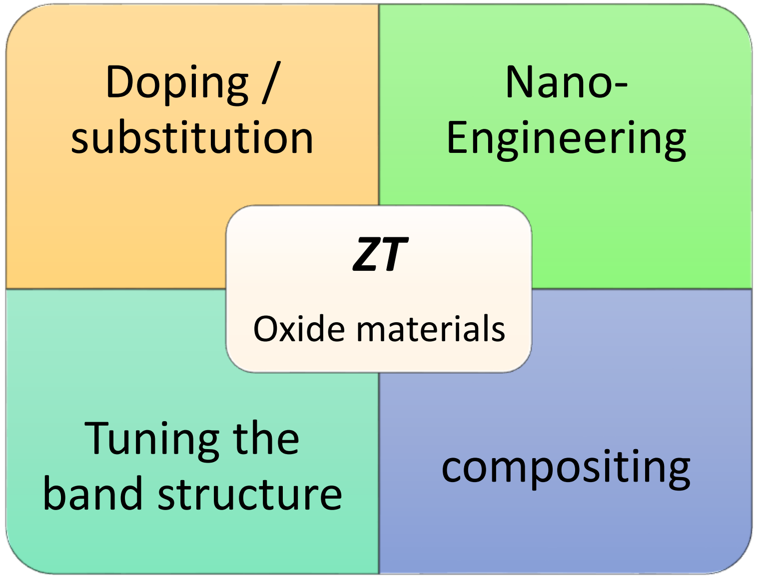

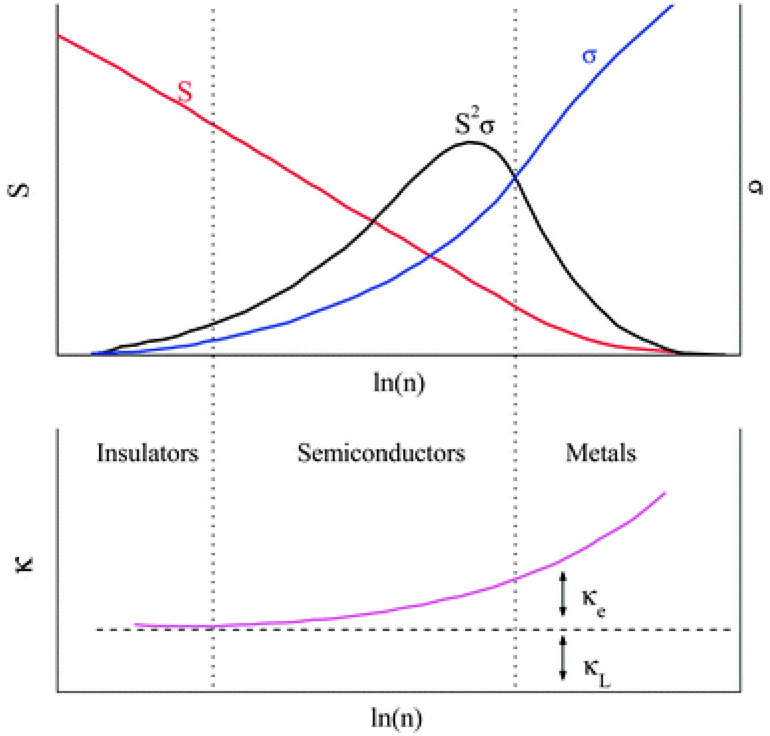

Wanqing Dong et al, *Metals* **2018**, *8*(10), 781

Transition metal oxides - Thermoelectric properties

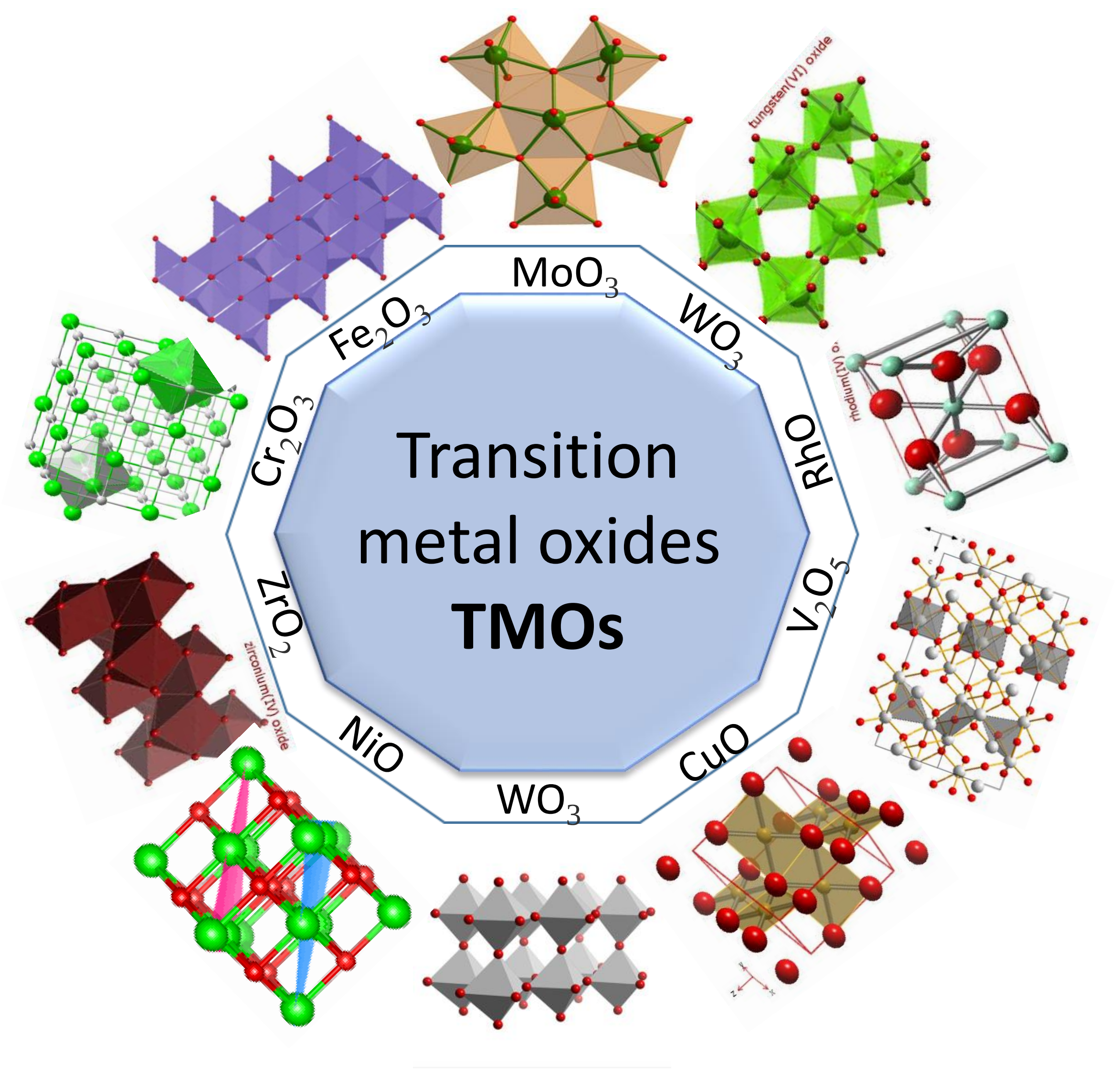

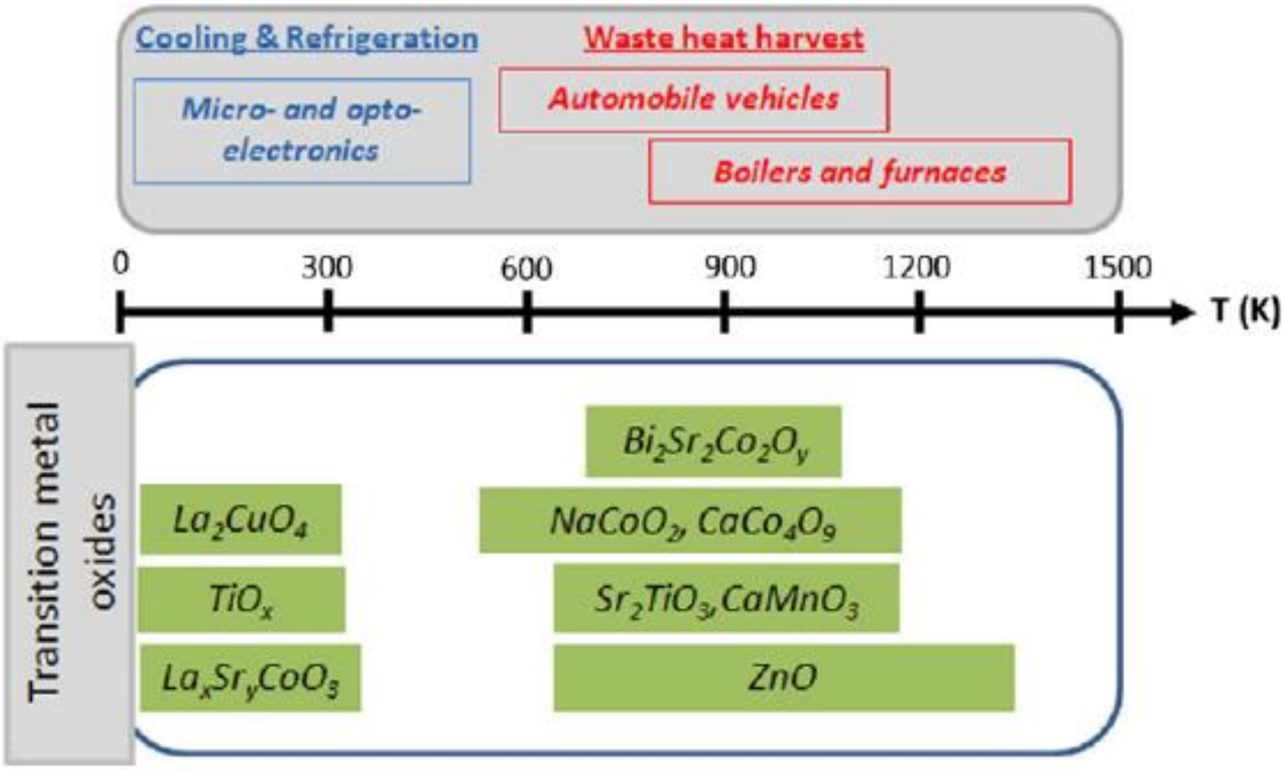

Operating temperature ranges of various TMOs and TMO composites

Sumeet Walia et al , *Progress in Materials Science* 58(8), **2013**,1443–1489.

Titanium oxides – TiO_x

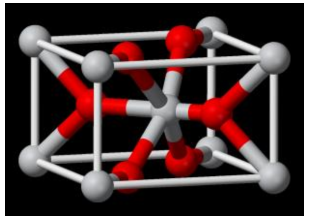

- **Stoichiometric TiO_2**
- Rutile and anatase exhibit a tetragonal structure
- ZT in pure TiO_2 is low <0.025

- **Non-stoichiometric TiO_x**
- ZT (<0.1).

- **Doped TiO_2**
- 2% Nb doped, anatase, n-type TiO_2 ZT~0.25

- **TiO_2 composite**
- Strontium titanate ($SrTiO_3$),
- $SrTi_{0.8}Nb_{0.2}O_3$ ZT~ 0.5

Manganese oxides – MnO_x

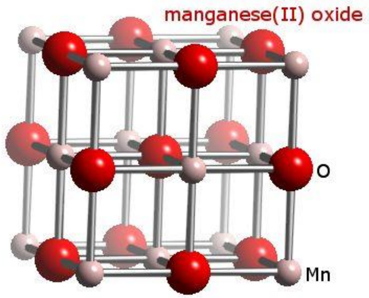

- α-MnO_2 (monoclinic structure) and β-MnO_2 (rutile structure)

- **Doping and compositing are good strategies for high ZT of MnO_x**

- perovskite type $CaMnO_3$. ZT > 0.1
- $CaMn_{0.96}Nb_{0.4}O_3$ ZT ~ 0.2

Cobalt oxides

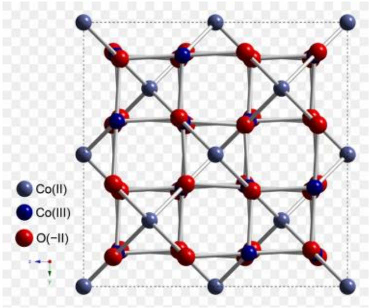

- Two stable oxide compounds: Co_3O_4 and CoO
- cubic lattice

- **Rare-earth cobalt oxides ($RECoO_3$)**
- Na_xCoO_2 ZT~0.75
- **Layered cobaltates**
- $Ca_3Co_4O_9$ ZT~0.3

Sumeet Walia et al , *Progress in Materials Science* 58(8), **2013**,1443–1489.

Zinc oxides – ZnO

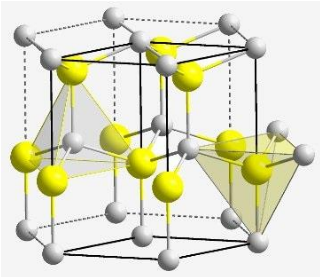

- Hexagonal - wurtzite, Cubic- zinc -blende.
- Nano structured Al-ZnO ZT~0.44
- $Zn_{0.985}Ga_{0.015}O$ ZT~0.25
- $Zn_{0.96}Al_{0.02}Ga_{0.02}O$ ZT~0.65

Copper oxides – Cu_2O and CuO

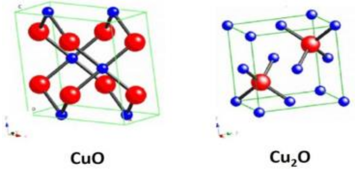

- Cubic crystal structure
- La_2CuO_4 ZT~0.06
- $La_{1.98}Y_{0.02}CuO_4$ ZT~0.17

Molybdenum oxides:-MoO_x

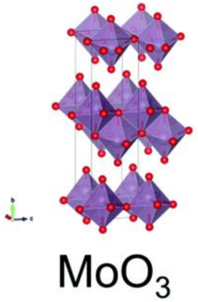

- α-MoO_3 - orthorhombic
  β-MoO_3 - monoclinic
- (RMo_8O_{14})
- where R = La, Ce, Nd and Sm
- $NdMo_8O_{18}$ ZT~0.1

Less explored TMOs

- Tungsten oxides:- ZnO,MnO_2, LiO_2 and TiO_2 doped WO_3
- Vanadium oxides:- $Na_xV_2O_5$
- Rhodium oxides:- K_xRhO_2
- Iron oxides:-$Li_xFe_{2-x}O_3$,Fe_2O_3/NiO
- Chromium oxides –Cr_2O_3,$CuCrO_2$
- Scandium oxides:- $CuScO_2$
- Zirconium oxides:- ZrO_2/$CoSb_3$
- Nickel oxides:- Li-NiO,Na-NiO
- Cadmium oxides:- CdO
- Iridium oxides:- Ca–Ir–O composite

Other transition metals are usually employed as dopants in other TE TMOs for tuning their various TE properties in order to achieve higher ZTs.

Sumeet Walia et al , *Progress in Materials Science* 58(8), **2013**,1443–1489.

p-type thermoelectric oxide

Layered cobaltates

Doping with substitutional elements

- -alkaline earth metals- Sr, Ba, and Mg
- -or rare-earth elements for Ca-site- La,Y,Sc
- -transition metal elements for Co-site.

$Ca_3Co_{4-x}M_xO_9$ (M = Fe, Cu, Mn, Ni, Ti, Cr, Cd, Nb, Ag)

Other doping elements, such as Bi and Na.

Dual doping/co-doping,

- -co-doped with Ag & Lu, La&Fe

n-type oxide TE materials,

the commonly used materials include

- -doped zinc oxide
- -perovskite-type doped strontium titanate or electron-doped $SrTiO_3$
- -calcium manganite

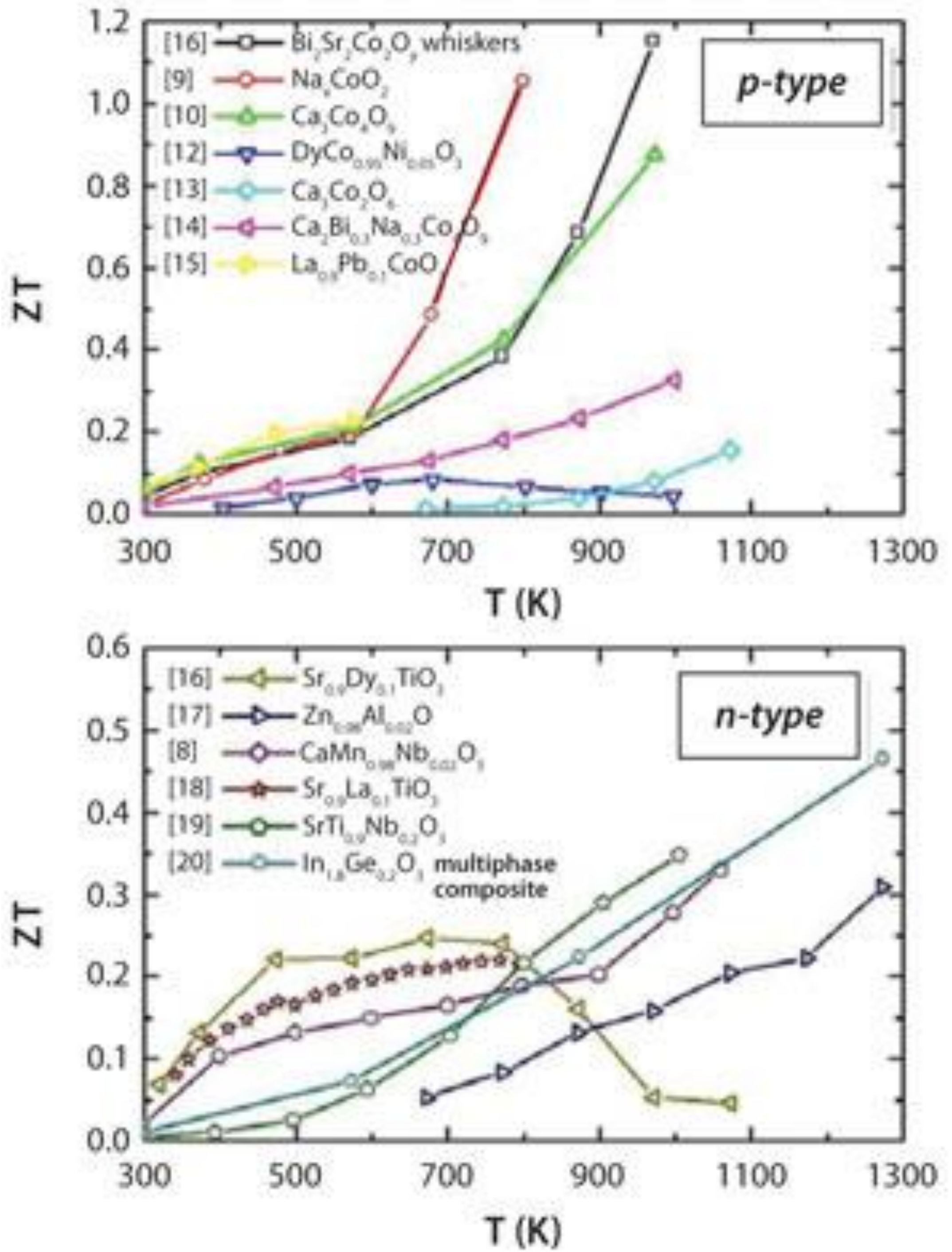

Architectures of TE Devices

Flat Bulk TE Device

Oxide-Based Thermoelectric Generator
Using p-type $Ca_3Co_4O_9$ and n-type $In_{1.95}Sn_{0.05}O_3$Legs

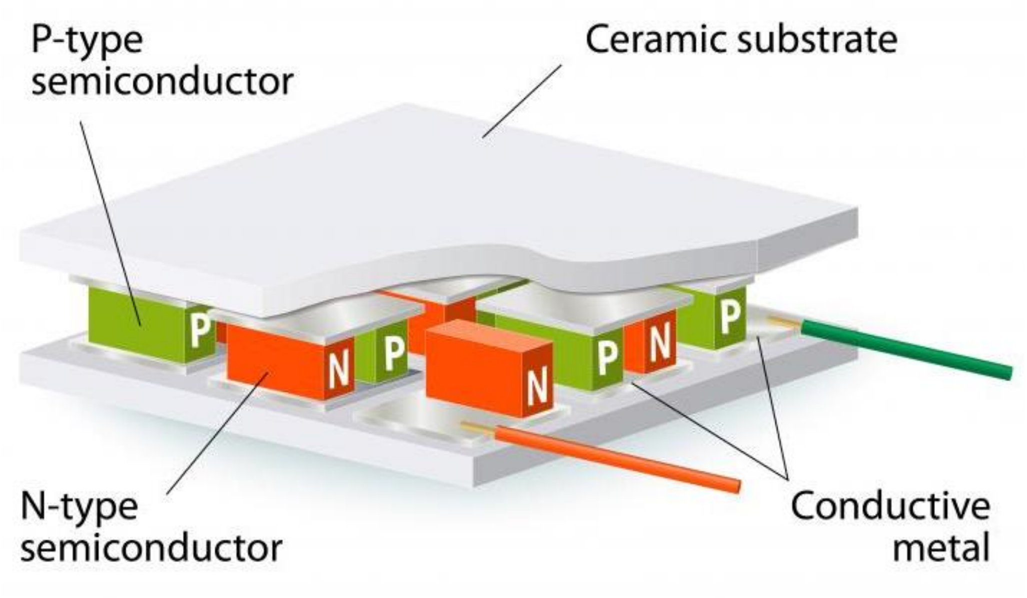

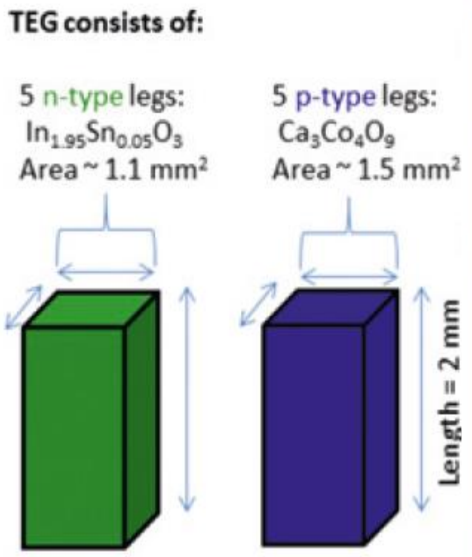

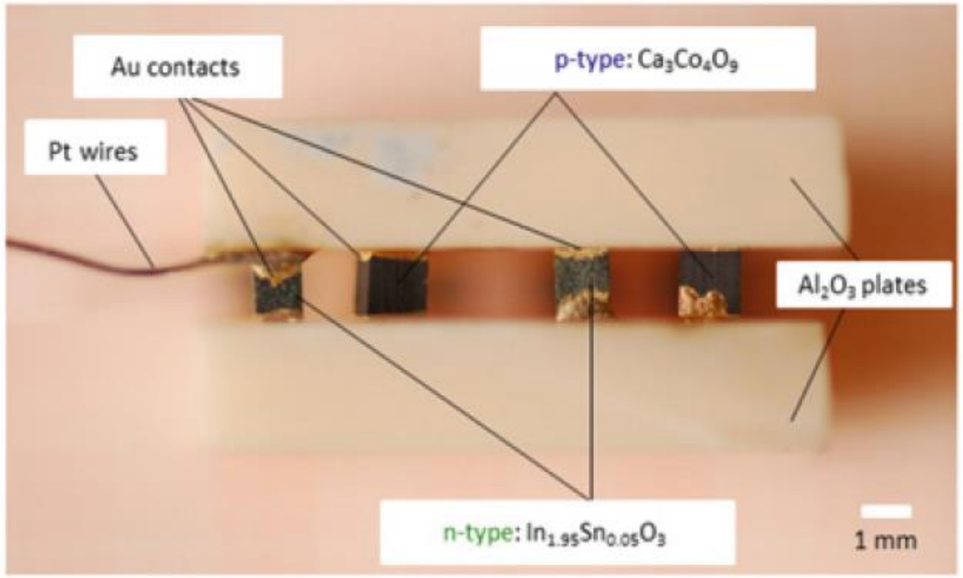

4.8 mW maximum power output

M. Bittner et al Energy Harvesting and Systems ***2016***

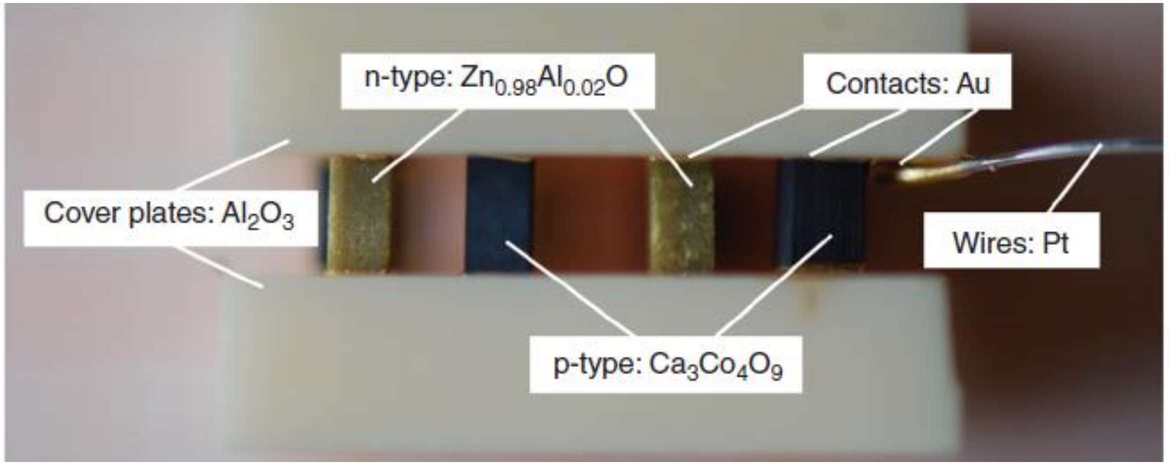

T_{hot}/K	ΔT/K	$R_{module} = R_{load}/\Omega$	P_{max}/mW	$I(P_{max})$/mA	$U(P_{max})$/mV	U_{OC}/mV	I_{SC}/mA	zT
1,023	200	65.40	0.55	2.94	189	379	5.79	0.10

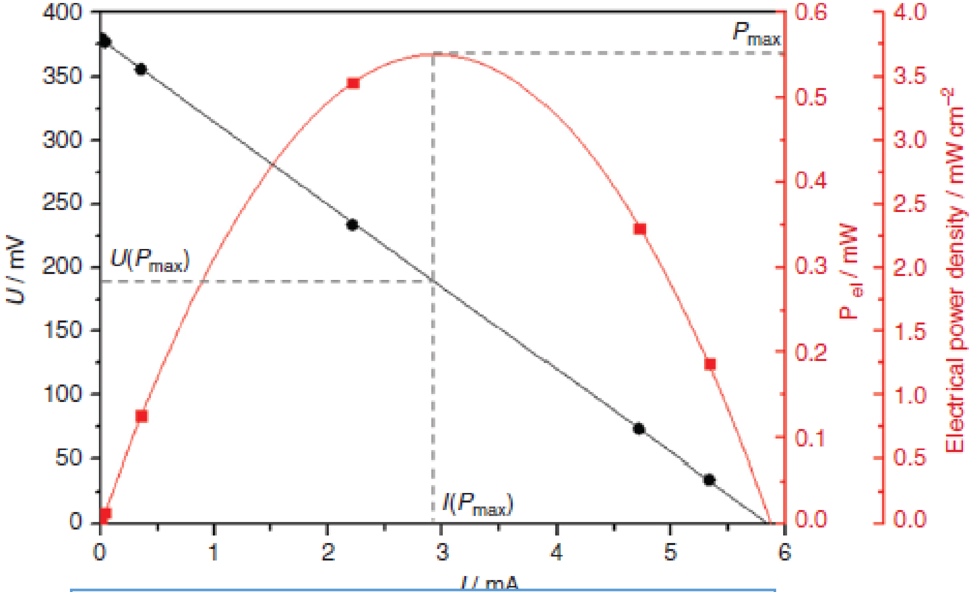

0.55mW maximum power output

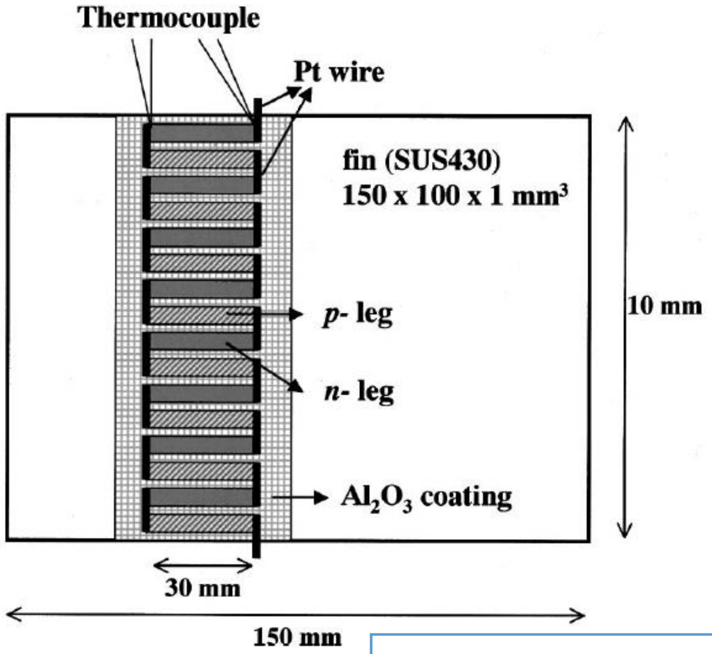

Materials	ρ-T	S (700 °C) μV/K	ρ (700 °C) mΩ cm	S^2/ρ (700 °C) 10^{-4}W m^{-1} K^{-2}
$Ca_{2.75}Gd_{0.25}Co_4O_9$ (p leg)	Semiconducting	185	7.8	4.8
$Ca_{0.92}La_{0.08}MnO_3$ (n leg)	Metallic	−120	6.6	2.2

Condition	T_h, °C	ΔT, °C	V_o, mV	P_{max}, mW
a	477	235	550	19.8
b	580	290	694	31.8
c	672	335	838	46.5
d	773	390	988	63.5

63.5 mW maximum power output

Matsubara et al *Appl. Phys. Lett.*, Vol. 78, No. 23, (**2001**)

Module materials	No. *p-n* couples	T_{hot} (K)	ΔT (K)	V_0 (V)	P_{max} (mW)	Legs-size (mm)	Power density (mW/cm^2)
p-$Ca_{2.7}Bi_{0.3}Co_4O_9$ *n*-$Ca_{0.92}La_{0.08}MnO_3$	8	773	390	0.9	63.5	3 × 3	44.1
p-$Ca_{2.7}Bi_{0.3}Co_4O_9$ *n*-$La_{0.9}Bi_{0.1}NiO_3$	140	1072	551	4.5	150	1.3 × 1.3 × 5	31.7
p-$NaCo_2O_4$ *n*-$Zn_{0.98}Al_{0.02}O$	12	839	462	0.8	58	3 × 4 × 10	20.1
p-$Ca_{2.7}Bi_{0.3}Co_4O_9$ *n*-$CaMn_{0.98}Mo_{0.02}O_3$	8	897	565	1	170	5 × 5 × 4.5	42.5
p-$Ca_{2.7}Bi_{0.3}Co_4O_9$ *n*-$CaMn_{0.98}Mo_{0.02}O_3$	8	1273	975	0.7	340	5 × 5 × 4.5	85
p-$NaCo_2O_4$ *n*-$Zn_{0.98}Al_{0.02}O$	12	934	455	0.8	52.5	3 × 4 × 10	18.2
p-$Ca_3Co_4O_9$ *n*-$(ZnO)_7In_2O_3$	44	1100	673	1.8	423	*p*:15 × 15 × 27 *n*:15 × 15 × 18	2.1
p-$Ca_{2.76}Cu_{0.24}Co_4O_9$ *n*-$Ca_{0.8}Dy_{0.2}MnO_3$	4	937	321	0.28	31	7 × 9 × 25	6.2
p-$Ca_3Co_4O_9$ *n*-$Zn_{0.98}Al_{0.02}O$	6	773	248	0.12	2.26	4 × 4 × 10	1.2
p-$Ca_3Co_4O_9$ *n*-$Zn_{0.98}Al_{0.02}O$	4	1173	700	0.67	256	4 × 4 × 8	2

Implementation in Thermoelectric devices

Segmented thermoelectric modules.

Combining different TE materials having different operation temperatures increases overall TE device performance .

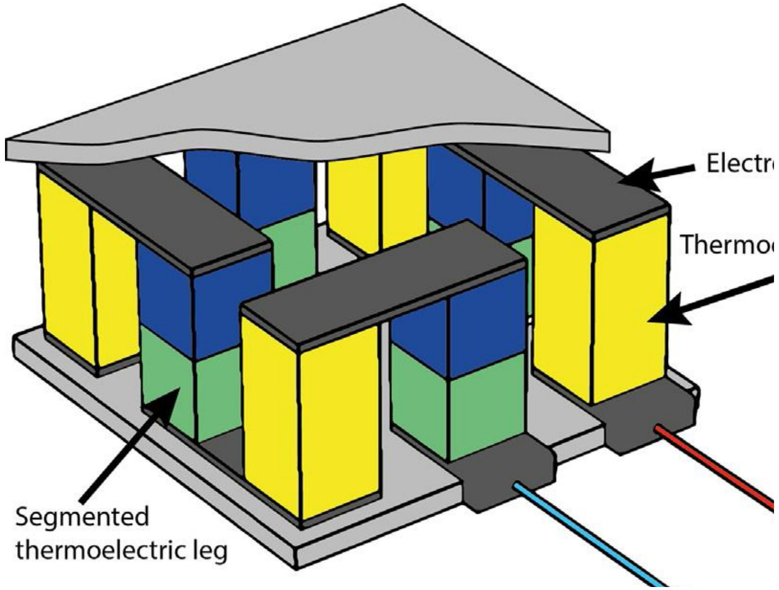

Module materials	T_{hot} (K)	ΔT (K)	Eff. (%) Cal.	Eff. (%) Exp.	Reference
p-$Ce_{0.9}Fe_{3.5}Co_{0.5}Sb_{12}$/ $Yb_{14}MnSb_{11}$ n-$CoSb_3$/$La_{3-x}Te_4$	1246	773	–	15	Fleurial et al. (2013)
p-$Bi_xSb_{2x}Te_3$/ $Ag_{0.9}Pb_9Sn9Sb_{0.6}T_{20}$ n-$Bi_2Te_{3x}Se_x$/ $Ag_{0.86}Pb_{19+x}SbTe_{20}$	670	358	9	6.56	D'Angelo et al. (2011)
p-Bi_2Te_3/PbTe n-Bi_2Te_3/TAGS	803	510	–	10	Crane et al. (2009)
p-Bi_2Te_3/$CeFe_4Sb_{12}$ n-Bi_2Te_3/$CoSb_3$	885	569	12	5.5	El-Genk and Saber (2003)
p-HH/$Ca_3Co_4O_9$ n-$Zn_{0.98}Al_{0.02}O$	1173	700	–	1.1	Hung et al. (2015a)

Nini Pryds, *Advanced Ceramics for Energy Conversion and Storage*, *Energ.Technol*. 3(11), **2015** , 1143–1151.

Bulk TEGs with pyramidal legs

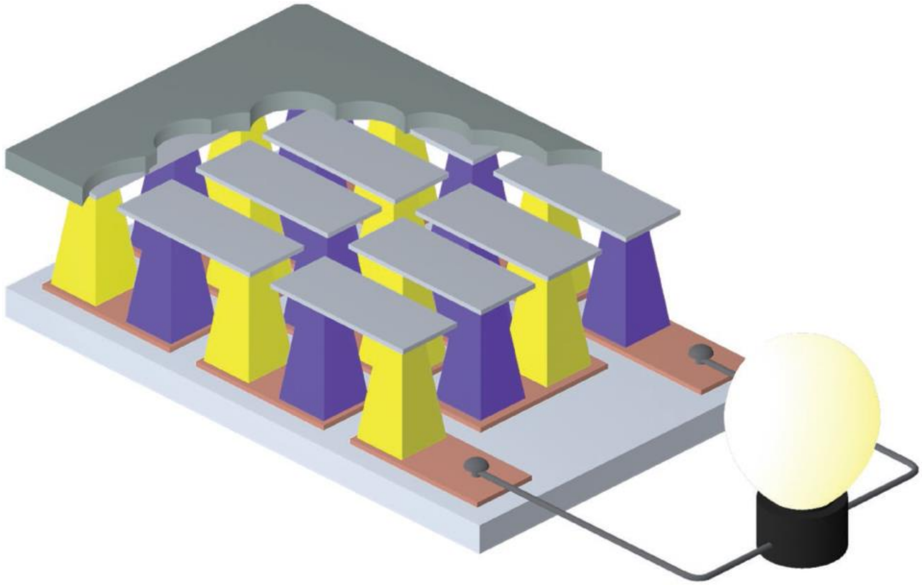

- Pyramidal legs help lowering the thermal conductance of the device increase the temperature gradient along the leg,
- Harnessing the Thomson effect that is largely ignored in the traditional (cuboid) structure.
- The measured output power shows ~70% proving the importance of geometrical configuration of the TE legs in the device performance.

Cylindrical-shaped TE devices

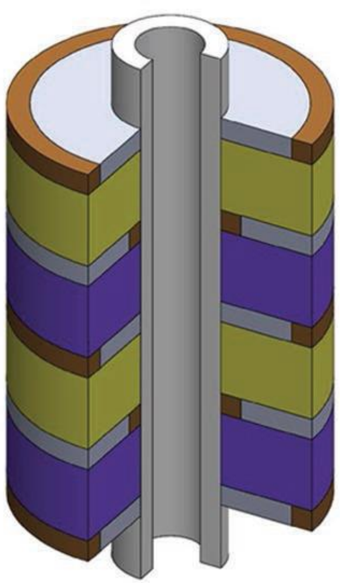

This design is advantageous for applications such as oil pipelines, cooling channels for power station transformers, vehicle exhaust pipe, etc., where the heat flow is in the radical direction

Adv. Mater. Technol. **2018**, *3*, 1700256

Unileg thermoelectric device

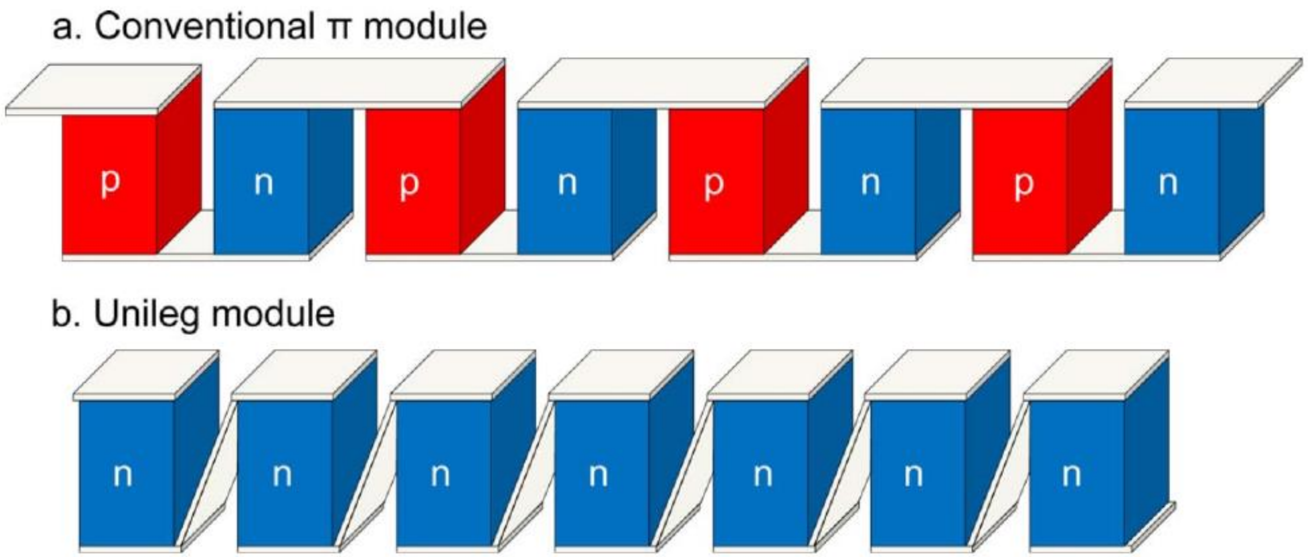

- ✓ Compatibility factor approach is not needed
- ✓ Simplifies the process and consequently reduces the cost
- ✓ Reduces problems of thermal expansion mismatch
- ✓ Reduce design restrictions
- ✓ Silver strips go from the bottom to the top of bars.

$Ca_{0.95}Sm_{0.05}MnO_3$ unileg thermoelectric device

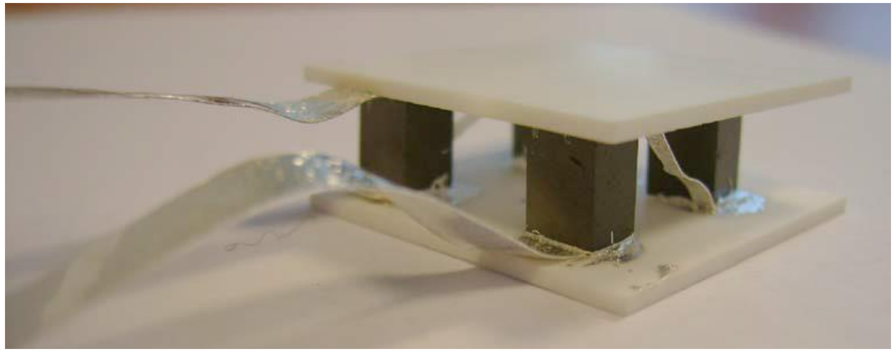

maximum power output for this four-leg device is16 mW

$Ca_{0.92}La_{0.08}MnO_3$ unileg thermoelectric device

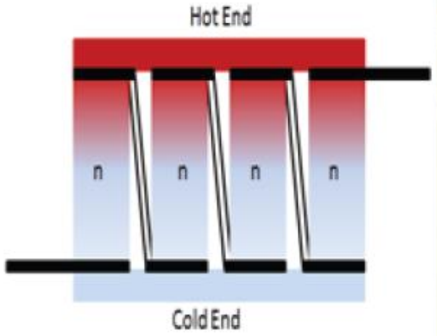

maximum power output for this nine-leg device is 50 mW

DAE Solid State Physics Symposium **(2016)**
J. Appl. Phys. 104, 014505 (**2008)**

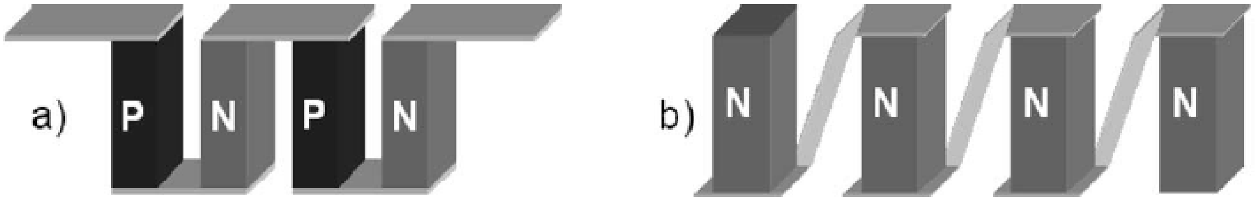

Differences between conventional thermoelectric device and *n*-type unileg module

Name	Materials	Type	Nb couple	Power (W)	MF
conventional	$Ca_{2.7}Bi_{0.3}Co_4O_9/La_{0.9}Bi_{0.1}NiO_3$	*pn*	1	0.03	0.15
conventional	$(Li)NiO/(Ba,Sr)PbO_3$	*pn*	2	0.034	0.3
conventional	$(Gd)Ca_3Co_4O_9/(La)CaMnO_3$	*pn*	8	0.089	0.82
conventional	$Ca_3Co_4O_9/Ca_{0.95}Sm_{0.05}MnO_3$	*pn*	2	0.031	0.57
Unileg	$Ca_{0.95}Sm_{0.05}MnO_3/Ca_{0.95}Sm_{0.05}MnO_3$	*n*	2	0.016	0.15

Lemonnier *et al.J. Appl. Phys*. 104, 014505 (**2008**).

pn-junction-based TEGs

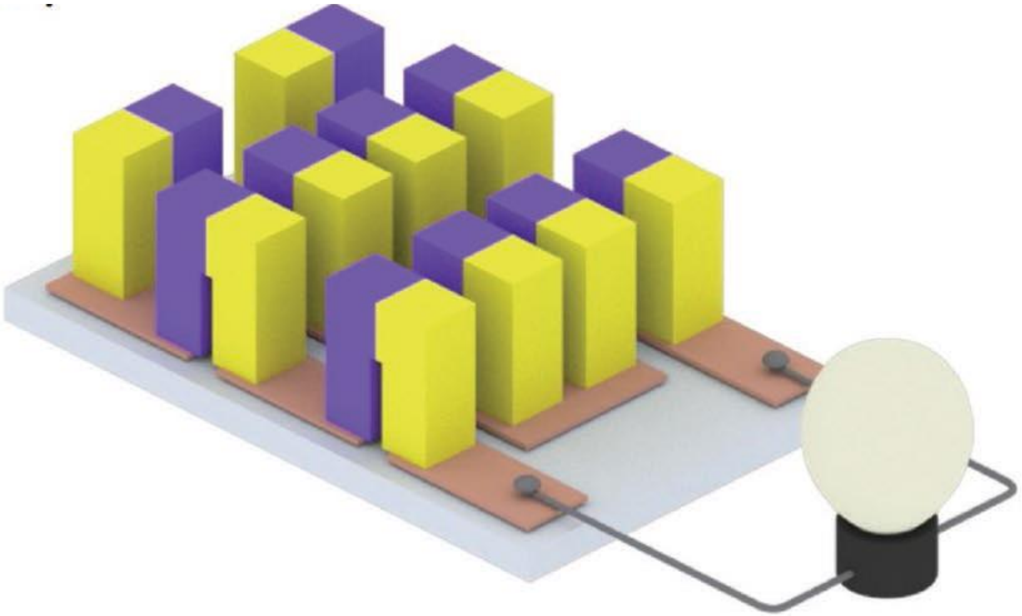

- Eliminate hot-side metallization completely
- Completely gets rid of contact issues between metal and semiconductor

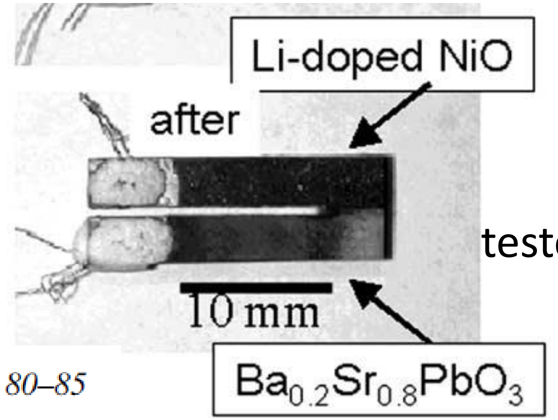

tested element

W. Shin et al. / Journal of Power Sources 103 (2001) 80–85

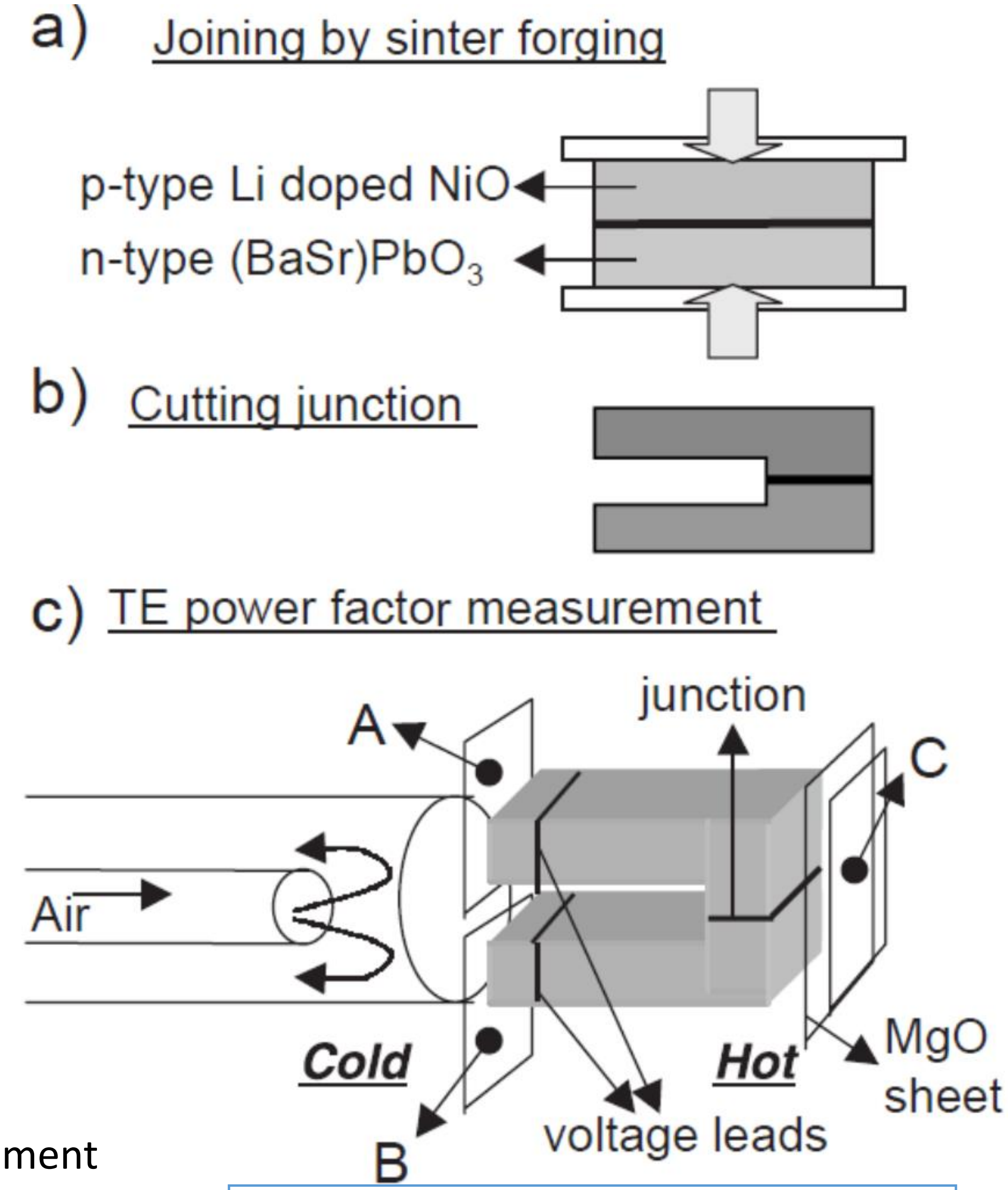

The output power was 14mW

Thin- and Thick-Film TE Devices

Micro-thermoelectric generators (μ-TDGs)

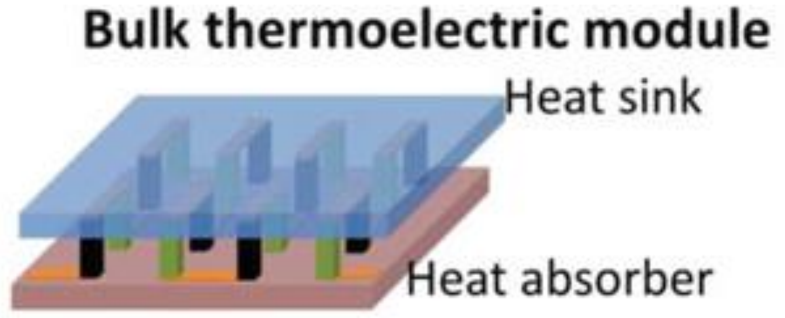

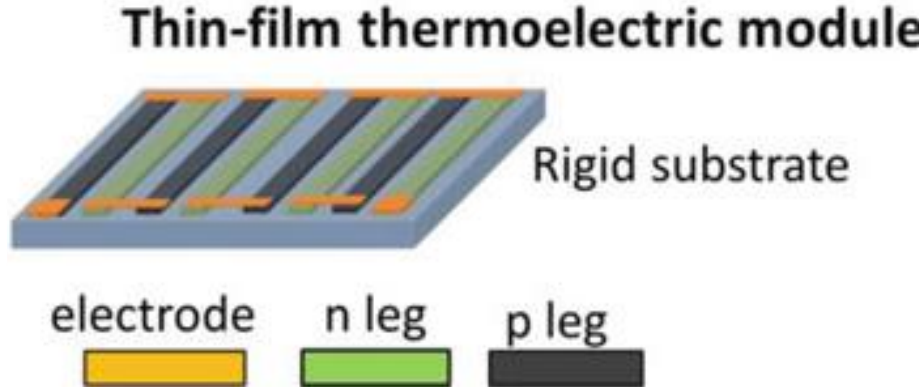

W. Somkhunthot, *Energy Procedia* 61, 795 (**2014**)
S. Saini, *Energ. Conv. Manag* 114, 251 (**2016**)

Thermoelectricity of p-CCO and n-ZAO thin films

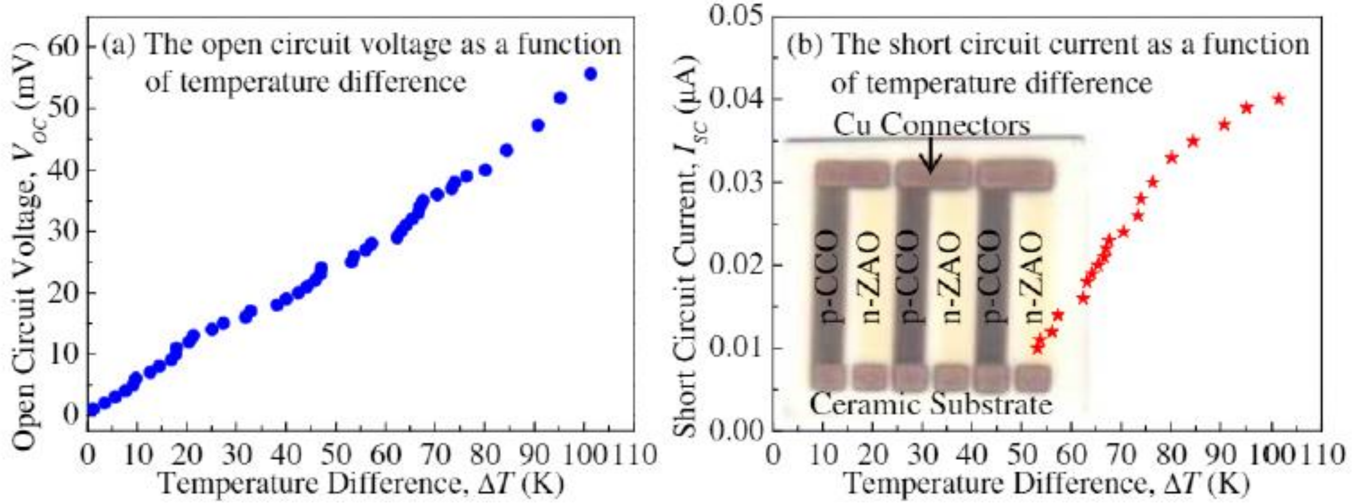

Thin-film module based on AZO and $CaCo_4O_9$

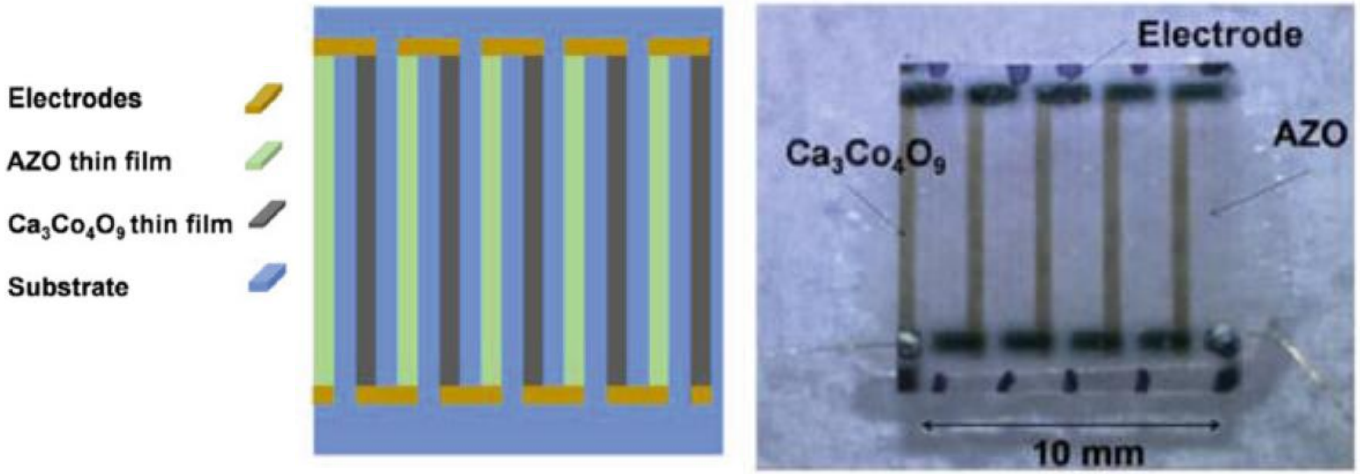

Thermoelectric Modules Based on Oxide Thin Films

n-Type	p-Type	Contacts	Number of legs (n + p)	Deposition technique	Size of a single leg	Sub.	Sub. size (mm L × mm W)	ΔT (°C)	Output power
Al-ZnO	$Ca_3Co_4O_9$	Cu	4 + 4	DC sputtering	20 mm × 3 mm × 440 nm t	Glass	25.0 × 50.0	78	N/A
Al-ZnO	$NaCoO_2$	Cu	3 + 3	DC sputtering	20 mm × 3 mm × 600 nm t	Al_2O_3	25.0 × 50.0	79.3	N/A
ZnO	CuO	Direct overlap	5 + 5	PVD	20 mm × 1 mm × 1000 nm t	Al_2O_3	20.0 × 20.0	16	102pW[a]
Al-ZnO	$Ca_3Co_4O_9$	Au	5 + 5	PLD	8 mm × 3 mm × 300 nm t	Glass	10.0 × 10.0	230	0.3 pW
Al-ZnO	$Ca_3Co_4O_9$	Au	5 + 5	PLD	8 mm × 3 mm × 300 nm t	$SrTiO_3$	10.0 × 10.0	230	16 pW
Al-ZnO	$Ca_3Co_4O_9$	Au	5 + 5	PLD	8 mm × 3 mm × 300 nm t	Al_2O_3	10.0 × 10.0	230	29.9 pW
Al-ZnO	N-Cu_xO	Ag	8 + 8	Spray pyrolysis	N/A	Glass	12.7 × 6.4	28	N/A
Al_2O_3/ZnO	$Bi_{0.5}Sb_{1.5}Te_3$	Ti/Au	4 + 4	ALD (n)/ sputtering (p)	8 mm × 3 mm × 200 nm t	Si/SiO_2	20.0 × 15.0	80	1 nW
$(ZnO)_5In_2O_3$	Pt	Pt	10 + 10	Screen printing	N/A	N/A	260 × 176	N/A	N/A
Pd/Ag	$Ca_3Co_4O_9$	Pd/Ag	10 + 10	Screen printing	N/A	N/A	260 × 176	N/A	N/A
Au	$CuCrO_2$:3% Mg	Au	3 + 3	RF sputtering	100 nm t[c]	Glass	25.0 × 25.0	170	10.6 nW

Mele, P., Saini, S., & Magnone, E. (**2019**). *Thermoelectric Thin Films*, 139–156.

Commercial products

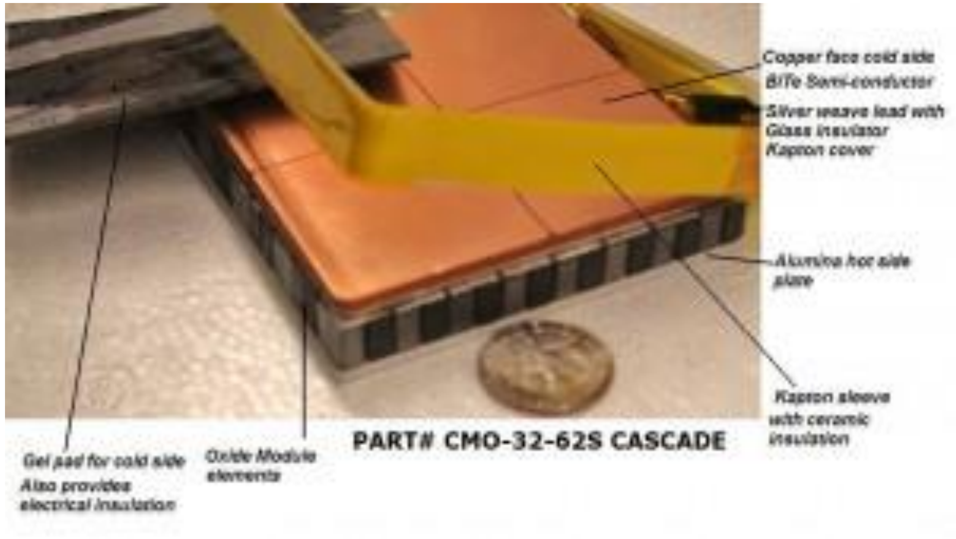

Available high temperature:

•Calcium/Manganese (CMO) TEG modules up to 800°C hot side CMO ONLY!

•Cascade (High Temperature (CMO) bonded with $Bi2Te3$ cold side. Up to 600°C

•These are the first Cascade Thermoelectric TEG modules ever to be available commercially hot side up to 600°C.

•Introducing a new Cascade design that works up to 750 °C available soon check back on a regular basis!

•CMO materials are extremely stable and will last up to 50 years with little or no degradation. They are the first high temperature material in this temperature range to be offered in the last 40 years!

Size:

•65 mm x 65 mm – 64 element design with 32 P & N-type Couples